Lignin nanoparticle-decorated nanocellulose cryogels as adsorbents for pharmaceutical pollutants

Agustin, Melissa B.

2023-03-15

Agustin , M B , Lehtonen , M , Kemell , M , Lahtinen , P , Oliaei , E & Mikkonen , K S 2023 , ' Lignin nanoparticle-decorated nanocellulose cryogels as adsorbents for pharmaceutical pollutants ' , Journal of Environmental Management , vol. 330 , 117210 . https://doi.org/10.1016/j.jenvman.2022.1172

http://hdl.handle.net/10138/356787
https://doi.org/10.1016/j.jenvman.2022.117210

Journal of Environmental Management 330 (2023) 117210

Contents lists available at ScienceDirect

Journal of Environmental Management

journal homepage: www.elsevier.com/locate/jenvman

Research article

Lignin nanoparticle-decorated nanocellulose cryogels as adsorbents for pharmaceutical pollutants

Melissa B. Agustin [a,*], Mari Lehtonen [a], Marianna Kemell [b], Panu Lahtinen [c], Erfan Oliaei [d], Kirsi S. Mikkonen [a,e]

[a] Department of Food and Nutrition, Faculty of Agriculture and Forestry, P.O. Box 66, FI-00014, University of Helsinki, Finland
[b] Department of Chemistry, Faculty of Science, P.O. Box 55, FI-00014, University of Helsinki, Finland
[c] VTT, Technical Research Centre of Finland, P.O. Box 1000, FIN-02044, VTT, Finland
[d] Department of Fiber and Polymer Technology, KTH Royal Institute of Technology, SE-100 44, Stockholm, Sweden
[e] Helsinki Institute of Sustainability Science, P.O. Box 65, FI-00014, University of Helsinki, Finland

ARTICLE INFO

Keywords:
Nanocellulose
Lignin nanoparticles
Cryogels
Adsorption
Pharmaceutical pollutants
Multi-component

ABSTRACT

Adsorption is a relatively simple wastewater treatment method that has the potential to mitigate the impacts of pharmaceutical pollution. This requires the development of reusable adsorbents that can simultaneously remove pharmaceuticals of varying chemical structure and properties. Here, the adsorption potential of nanostructured wood-based adsorbents towards different pharmaceuticals in a multi-component system was investigated. The adsorbents in the form of macroporous cryogels were prepared by anchoring lignin nanoparticles (LNPs) to the nanocellulose network via electrostatic attraction. The naturally anionic LNPs were anchored to cationic cellulose nanofibrils (cCNF) and the cationic LNPs (cLNPs) were combined with anionic TEMPO-oxidized CNF (TCNF), producing two sets of nanocellulose-based cryogels that also differed in their overall surface charge density. The cryogels, prepared by freeze-drying, showed layered cellulosic sheets randomly decorated with spherical lignin on the surface. They exhibited varying selectivity and efficiency in removing pharmaceuticals with differing aromaticity, polarity and ionic characters. Their adsorption potential was also affected by the type (unmodified or cationic), amount and morphology of the lignin nanomaterials, as well as the pH of the pharmaceutical solution.

Overall, the findings revealed that LNPs or cLNPs can act as functionalizing and crosslinking agents to nanocellulose-based cryogels. Despite the decrease in the overall positive surface charge, the addition of LNPs to the cCNF-based cryogels showed enhanced adsorption, not only towards the anionic aromatic pharmaceutical diclofenac but also towards the aromatic cationic metoprolol (MPL) and tramadol (TRA) and neutral aromatic carbamazepine. The addition of cLNPs to TCNF-based cryogels improved the adsorption of MPL and TRA despite the decrease in the net negative surface charge. The improved adsorption was attributed to modes of removal other than electrostatic attraction, and they could be π-π aromatic ring or hydrophobic interactions brought by the addition of LNPs or cLNPs. However, significant improvement was only found if the ratio of LNPs or cLNPs to nanocellulose was 0.6:1 or higher and with spherical lignin nanomaterials. As crosslinking agents, the LNPs or cLNPs affected the rheological behavior of the gels, and increased the firmness and decreased the water holding capacity of the corresponding cryogels. The resistance of the cryogels towards disintegration with exposure to water also improved with crosslinking, which eventually enabled the cryogels, especially the TCNF-based one, to be regenerated and reused for five cycles of adsorption-desorption experiment for the model pharmaceutical MPL. Thus, this study opened new opportunities to utilize LNPs in providing nanocellulose-based adsorbents with additional functional groups, which were otherwise often achieved by rigorous chemical modifications, at the same time, crosslinking the nanocellulose network.

* Corresponding author.
E-mail address: melissa.agustin@vtt.fi (M.B. Agustin).

https://doi.org/10.1016/j.jenvman.2022.117210
Received 12 October 2022; Received in revised form 30 December 2022; Accepted 31 December 2022
Available online 5 January 2023

1. Introduction

Clean water is one of the foundations of a sustainable society. It plays a vital role in maintaining public health, as drinking water or water for daily use, and as an indispensable resource for the food industry (Bhagwat, 2019). Thus, global accessibility to clean water is among the 2030 UN sustainable development goals (UNSDG 6). The delivery of this goal is hampered by the problems posed by emerging water contaminants, including pharmaceutical pollutants.

Pharmaceutical pollutants are the residual active pharmaceutical ingredients (APIs) or their transformation products found at varying levels in natural matrices. Globally, 613 APIs or their metabolites have been detected above their respective detection limits in liquid effluents, which include treated municipal, industrial or hospital wastewaters and veterinary emissions from aquaculture or livestock (Dusi et al., 2019). Even though they are present at relatively low concentrations (ng or μg per liter), they pose serious threats to humans and aquatic biota because of their potent bioactivity even at very low doses (BIO Intelligence Service, 2013). Moreover, because of the continuous influx of pharmaceutical pollutants, mostly from municipal wastewaters, they accumulate in the environment and create a "complex pharmaceutical pool", which could exert higher ecotoxicity than that of the individual APIs (Ebele et al., 2017). In order to mitigate the impacts of pharmaceutical pollution, regulating this influx from municipal wastewater treatment plants is a crucial step. Improvement of wastewater treatment technologies to efficiently remove pharmaceutical residues from wastewaters is required.

Adsorption is one of the most commonly used wastewater treatment methods because of its simple operation, low energy consumption, and the absence of toxic byproducts (De Andrade et al., 2018; Rashed, 2013; Rivera-Utrilla et al., 2013). Adsorption units are either located before biological treatment to remove toxic compounds or after physico-chemical treatment to remove micropollutants (Ahmed et al., 2022). Adsorption utilizes solid adsorbents that can hold the target contaminants via physical and/or chemical intermolecular interactions. Activated carbon (AC), either in powdered or granular form, is the typical adsorbent used in many water treatment facilities. However, despite the relatively high efficiency of AC, there is a continuous effort to find alternatives to AC because of its expensive regeneration method and significant loss during regeneration (Crini et al., 2019). These efforts led to the development of non-conventional adsorbents produced from biological, industrial and agricultural products or by-products. Utilizing renewable materials to produce adsorbents is also a way to respond to the global call for sustainable production embodied in the UN Sustainable Development Goal 12.

Wood-derived cellulose and lignin are forestry products that have been well explored and proven to have immense potential in various applications. In their nanoscale forms, as nanocelluloses or lignin nanoparticles (LNPs), they exhibit unique properties, which have been exploited for advanced and diverse applications. For instance, the high mechanical properties and abundance of modifiable hydroxyls made nanocelluloses excellent materials for developing nanocomposites for tissue engineering, drug delivery, energy storage, filtration membranes, and others (Eichhorn et al., 2022). They are also feasible substrates for the manufacture of transparent lightweight flexible devices and sensors (Kontturi et al., 2018). Meanwhile, LNPs with their spherical shapes and polyaromatic structure have been found as great dispersants, and antimicrobial, antioxidant or UV-protecting agents in the formulation of coatings, adhesives and composites (Österberg et al., 2020). LNPs were also widely investigated as carriers for controlled delivery or release of bioactive ingredients (Sipponen et al., 2019).

Both nanocelluloses and LNPs are promising materials for developing adsorbents for wastewater treatment. In fact, nanocelluloses, especially their chemically-modified derivatives, in the form of hydrogels or aerogels, have been widely studied as adsorbents for oil, heavy metals, dyes, and a few pharmaceuticals (Aoudi et al., 2022). Spherical LNPs are not as well-explored as the nanocelluloses in terms of adsorption studies, but lignin derivatives and lignin-based carbon materials have shown efficiency in removing various types of pollutants from wastewater, including pharmaceuticals (Supanchaiyamat et al., 2019; Wang et al., 2022). So far, only our previous study has made a systematic investigation of the adsorption potential of various types of LNPs towards different pharmaceuticals (Agustin et al., 2022). We found that LNPs, either in its natural anionic or cationized form (cLNPs), adsorbed a wide range of pharmaceuticals, from charged to neutral, aromatic to non-aromatic, acidic to basic. Despite their promising performance as adsorbents, LNPs and cLNPs, however, cannot be used alone in large scale applications, because of their tendency to form colloidal suspension in water, making their removal after adsorption a challenge. Thus, in this current work, we anchored LNPs or cLNPs on a nanocellulose substrate to develop cellulose-based macroporous materials, which we have called cryogels. This is to be in accordance with the currently acknowledged term for porous cellulosic materials produced by freeze-drying (Buchtová et al., 2019). To our knowledge, this is the first attempt to combine spherical LNPs and nanocellulose in the preparation of macroporous wood-based cryogels as adsorbents for pharmaceuticals. We combined cationic cellulose nanofibrils (cCNF) with LNPs and the anionic TEMPO-oxidized cellulose nanofibril (TCNF) with cLNPs. Using different types of LNPs and nanocelluloses would enable identifying the combination that would cater the removal of pharmaceuticals having wide chemical variability. The formulation was based on opposite surface charges to enable the LNPs or cLNPs to anchor on the nanocellulose network via electrostatic attraction. The LNPs or cLNPs, with their polyaromatic structure bearing various types of functional groups such as carboxyls, phenolic and aliphatic hydroxyls, and methoxyls, are viewed to act as functionalizing agents that would enhance and widen the adsorption potential of the nanocellulose. Because of their differing charge with the respective nanocellulose they are attached to, the LNPs or cLNPs are also envisioned to act as crosslinking agents between the nananofibrils, strengthening the cryogels.

To determine the efficiency and selectivity of the nanocellulose-based cryogels as adsorbents, multi-component batch equilibrium adsorption tests were performed, wherein at least six pharmaceuticals with differing chemical structure, polarity, acidity or basicity, and ionic character were simultaneously present in the test solutions. This set-up is more representative of the cocktail of pharmaceuticals in wastewaters than the single-component system, which is most often used in adsorption studies. The cryogels were characterized and the factors affecting their adsorption potential including the type, amount and morphology of the LNPs, surface charge density of the cryogels, and pH of the surrounding medium were investigated. Finally, a series of adsorption-desorption experiments were performed to assess the reusability of the cryogels. The findings of this study is expected to provide new insights on the performance of LNPs or cLNPs as functionalizing agents and would be useful not only in designing future adsorbents but also in developing other types of bio-based functional materials for various applications, such as drug encapsulation and delivery.

2. Materials and methods

2.1. Materials

The TCNF was produced from the never-dried bleached Metsä Board's Husum softwood kraft pulp fibers which were initially mill-beaten, TEMPO-oxidized, washed, and mechanically nanofibrillated using a high-pressure microfluidizer at 1600 bar pressure (Microfluidizer M-110EH, Microfluidics Corp., USA) (Herrera et al., 2018). The cCNF with a degree of substitution of 0.35 was provided by VTT, Finland. It was produced by cationization of the hardwood kraft pulp by glycidyltrimetylammonium chloride (GTAC, Sigma-Aldrich, Finland), removal of unreacted reagents by repeated washing, followed by two passes through a microfluidizer at 1800 bar pressure (Skogberg et al.,

2017). The sulfur-free birch lignin with a carboxyl and phenolic content of 0.56 and 4.27 mmol/g (^{31}P-NMR method) produced by BLN method (von Schoultz, 2016) was obtained from CH Bioforce Oy (Finland). The pharmaceutical compounds, which are certified reference materials were all purchased from Sigma-Aldrich (Finland) and were used as received (Table S1). The antidiabetic drug metformin, MTF, is included in the 2022 EU watch list of priority substances selected for regular monitoring in the aquatic environment because of their potential risks (European Commission, 2022). The other six substances were in the list of top 20 pharmaceuticals measured in highest concentrations in effluents collected from municipal wastewater treatment plants in countries around the Baltic Sea region (UNESCO and HELCOM, 2017). Acetonitrile and methanol used for chromatographic analysis were of chromasolv grade. The cationic and anionic titrants were supplied by BTG Instrument, GmbH, Germany.

2.2. Preparation of the LNPs and cLNPs

The LNPs were prepared by acetone nanoprecipitation, which involves dissolution of lignin in aqueous 75% (v/v) acetone followed by rapid addition of water (Farooq et al., 2019; Figueiredo et al., 2021). The preparation of LNPs by ultrasonication followed the procedure we reported in previous work (Agustin et al., 2019). The cLNPs were produced by coating the LNPs with lignin cationized by GTAC at a dry mass ratio of cationic lignin to LNP of 0.3 (Agustin et al., 2022; Sipponen et al., 2017). The method for lignin cationization using GTAC is described by Kong et al. (2015).

2.3. Preparation of the cryogels

Two sets of cryogels were prepared: the cLNP/TCNF and the LNP/cCNF combinations. The gels were prepared by mixing a known mass of nanocellulose and LNP or cLNP suspensions, and adjusting with deionized water to obtain a 0.4% nanocellulose in the final gel composition. The gel was stirred overnight, cast on trays with cylindrical molds, allowed to stand for 5 h at 5 °C, and then frozen at −70 °C overnight. The frozen gels were freeze-dried for two days, obtaining the cryogels. The TCNF-based cryogels were named T0, T0.2, T0.4, T0.6, and T1.0, where the numbers represent the dry weight ratio of cLNP to TCNF. Following the same concept, the cCNF-based cryogels were designated as C0, C0.6, and C1.0.

2.4. Characterization of the gels and cryogels

Rheology. The rheological properties were measured in duplicates for each gel using a HAAKE MARS 40 rheometer (Thermo Scientific, Germany) within 24 h after gel preparation. All measurements were performed at 20 °C using a 35-mm diameter plate. The viscosity curves were obtained by performing a rotational program, in which the shear rate was increased step-wise from 0.3 s^{-1}–300 s^{-1}. The storage modulus (G′) and loss modulus (G″) were measured at an oscillation frequency range of 0.01–10 Hz within the linear viscoelastic range, which was determined from a strain sweep measurement.

Morphology. Atomic force microscopy (AFM) imaging was performed to visualize the morphology of the nanomaterials using the Multimode AFM Nanoscope 9 (Bruker, Germany). The PPP-FMaud-10 by Nanosensors with a spring constant of 0.5–9.5 N/m was used to probe the samples using the quantitative imaging mode program. The SEM images of the cryogels were acquired with a Hitachi S-4800 field emission scanning electron microscope (FESEM). The samples were coated with 5 nm of Au–Pd alloy prior to imaging, to make their surface conductive.

Texture analysis. The Texture Analyzer TA-XT2i (Stable Microsystems, Godalming, UK) was used to characterize the mechanical properties of the cryogels in compression mode. At least seven replicate cylindrical samples with diameters of 18.0 ± 1.0 mm and height of 13.7 ± 1.3 mm were kept at 50% relative humidity for 24 h prior the test. The samples were compressed to 50% of their initial height using a 36 mm aluminum cylindrical probe, force of 5.0 kg, a trigger force of 0.05 N, and hold time of 30 s. The pre-test speed and test speed were 1.0 mm/s and the post-test speed was 10 mm/s. From the force-time profile, the firmness and springiness were determined.

Bulk density. The bulk density was determined from the mass and volume data obtained by weighing with analytical balance and manual measurement of the height and diameter of cylindrical samples using a digital caliper, respectively. The height and diameter were measured from at least 5 different locations to get the average volume.

Water absorption capacity (WAC). Three pre-weighed cylindrical samples from each treatment were placed in individual vessels containing 35 mL water. The cryogels were kept in water for 3 h, checking regularly to ensure the samples were completely soaked. With a spatula the samples were then taken out from the water, and placed on top of an inverted cylindrical sieve with nylon mesh to allow the excess water to drip freely for about 30s per sample. The wet cryogels were weighed and the WAC was calculated as the ratio of the mass of absorbed water to the initial mass of the sample.

Charge density. The surface charge density of the cryogels was determined in duplicates by polyelectrolyte titration using the Mütek™ PCD-05 particle charge detector (BTG Instruments GmbH, Germany) coupled to an Omnis autotitrator (Methrohm Corp, Switzerland). A 10-mg sample of the cryogel was soaked in 10 mL milliQ water and adjusted to pH 6 by 0.1 M NaOH. An excess of a polyelectrolyte titrant of charge opposite to that of the cryogels (i.e. cationic 0.001 N PDADMAC for TCNF-based cryogels and anionic 0.001 N PESNa for cCNF-based cryogels) was added and the mixture was magnetically stirred overnight. The mixture was screen filtered and an aliquot was back-titrated either with PDADMAC or PESNa to determine the amount of excess polyelectrolyte.

2.5. Adsorption experiment

The adsorption experiment was carried out in a multi-component aqueous solution containing 20 mg/L of each API. This concentration was high enough to obtain samples with sufficient signal in the ultra-high performance liquid chromatography (UHPLC) analysis without the need for possible pre-concentration in the case of high removal rate. Although seven pharmaceuticals (Table S1) were investigated, only six APIs were tested at the same time because of the overlapping peaks of metoprolol (MPL) and tramadol (TRA) during chromatographic analysis. Two sets of analysis were done: a group with MPL and another group with TRA. The pH of the API solution was adjusted to pH 3 or 6 using 0.1 M HCl or 0.1 M NaOH, respectively. In a disposable borosilicate glass vial, a 1:1 ratio of the mass (mg) of the cryogel to the volume (mL) of the API solution was mixed and shaken on a reciprocating mechanical shaker (120 motions per minute) for 90 min, which was chosen based on a preliminary time-series experiment, wherein no change in adsorption behavior from 30 to 210 min contact time was observed (Fig. S1). After which, a 1-mL sample was withdrawn and filtered (0.45 μm, Acrodisc wwPTFE Membrane). At least three independent analyses, with random replications, were performed. To eliminate potential losses due to adsorption on the surfaces of materials, a blank containing only the APIs was prepared and analyzed for each analysis set. For the determination of maximum adsorption capacity, the same procedure was followed but using a single-component solution at varying concentrations from 5 mg/L to 300 mg/L and a contact time of 150 min. The fitting of adsorption data with various adsorption isotherm models (Langmuir, Freundlich and Sips) was done using Origin Lab (Massachusetts, USA).

2.6. Quantitation of active pharmaceutical ingredients

The amount of the residual APIs in water after the adsorption test was analyzed by UHPLC using the Waters Acquity UPLC system (Waters,

Milford, MA, USA) combined with UV/VIS detection (photodiode array) following the optimized procedure we used in our previous work (Agustin et al., 2022). Briefly, the conditions were: gradient elution in a reversed phase column (Acquity HSS T3 C18) with 0.1% formic acid and acetonitrile as mobile phases, flow rate of 0.4 mL/min, 6-min elution time, and calibration based on external standards.

2.7. Reusability test

A series of adsorption-desorption experiments were performed for the cryogel that showed the highest adsorption potential. First, different methods of desorption were tested which include a combination of shaking or ultrasonic treatment in water or 0.1 M HCl. After identifying the suitable desorption method, the selected cryogel was used for five cycles of adsorption-desorption while monitoring the percentage of removal to assess the efficiency of the cryogel for each cycle. After desorption, the cryogel was repeatedly rinsed with deionized water, pressed on a tissue paper to remove most of the absorbed water, and reused for the next adsorption. This approach is less costly than freeze-drying the cryogel after each cycle.

2.8. Statistical analysis

Adsorption data was subjected to a one-way ANOVA analysis at 5% significance by the Tukey test using Origin Lab.

3. Results and discussion

3.1. The nanomaterials and their gels

The appearance, structural representation, and morphology of each nanomaterial used in the preparation of the cryogels are shown in Fig. 1A–D. The nanocelluloses appear as a semi-transparent gel consisting of long, intertwined nanofibrils having widths of less than 10 nm and a length that can extend to a few micrometers. The TCNF is negatively charged because of the carboxylation at carbon 6 while the cCNF carries positively charged ternary ammonium groups (Fig. 1B). The LNPs and cLNPs form a brown colloidal suspension consisting of spherical nanoparticles (Fig. 1D). The unmodified LNPs are typically negatively charged exhibiting a zeta potential of less than −40 mV (Figueiredo et al., 2021). These LNPs can be cationized by coating the surface with cationic lignin, produced by reacting lignin with GTAC in alkaline conditions (Fig. 1C). Because each cationic lignin molecule can carry a number of positively charged ternary ammonium groups, it is possible to anchor the cationic lignin to LNPs while leaving the other cationic groups available on the surface, resulting in a positive zeta potential (+20 mV). The coating of cationic lignin only altered the surface charge of the LNPs but kept the shape of the particles as shown in Fig. 1D. A more detailed characterization of the LNPs and cLNPs used here is available in our previous publications (Agustin et al., 2022;Figueiredo et al., 2021).

The aqueous suspension of nanocelluloses naturally formed a gel because of the physically intertwined nanofibrils that allow them to form a three-dimensional network. All the gels produced from the mixing of nanocellulose with lignin nanomaterials of opposite charged

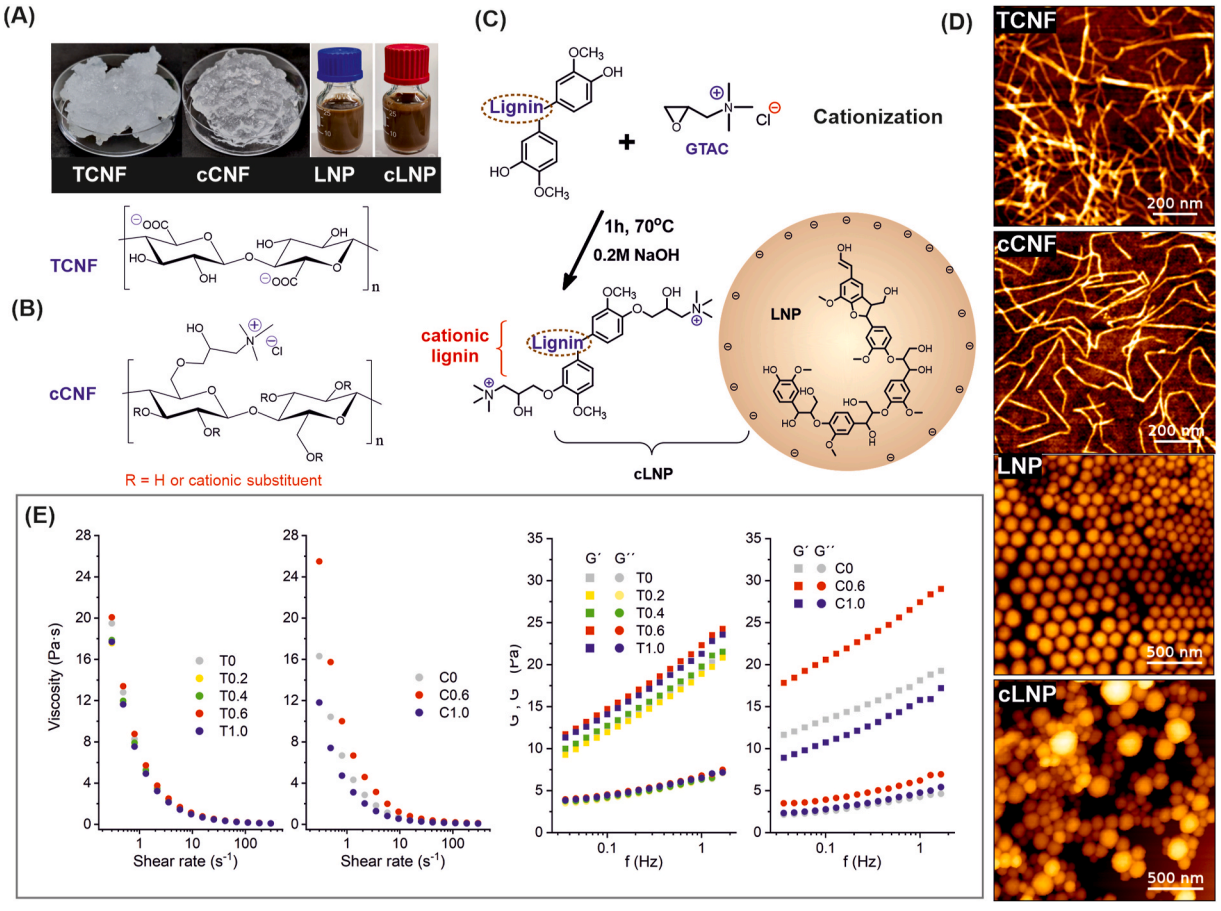

Fig. 1. The visual appearance (A), structure (B,C) and morphology (D) of the cellulose- and lignin-based nanomaterials and the viscoelastic properties of their gels produced at varying lignin to nanocellulose ratios (E).

displayed shear thinning behavior (Fig. 1E). At a similar solid content and at a shear rate of $0.3s^{-1}$, the pure TCNF gel had higher shear viscosity than the pure cCNF gel (19.5 against 16.3 mPa·s), an indication that the TCNF had longer fibrils than the latter, which was also supported by previous studies on rheological behavior of nanocellulose suspensions as affected by the nanofibril length (Moberg et al., 2017).

The addition of varying amounts of cLNPs in the TCNF suspension did not produce significant differences in the dynamic shear viscosity profiles. However, a different behavior was observed in the cCNF/LNP combinations, wherein the viscosity of C0.6 was much higher than that of the pure cCNF gel. This could be due to the difference in the fibril length between TCNF and cCNF. For TCNF gels consisting of long, intertwined nanofibrils, the addition of spherical cLNPs had little effect on the viscosity of the gels despite the formation of crosslinks between the particles and the fibrils. On the other hand, with shorter fibrils in cCNF, the crosslinking induced by the addition of LNPs greatly affected its viscosity.

All the gels exhibited viscoelastic properties, with a shear storage modulus (G′) higher than the loss modulus (G′′) (Fig. 1E). A stronger network characterized by an increase in G′ was observed with the addition of LNPs or cLNPs to the nanocellulosic gel. This was most apparent for C0.6, which can be attributed to the electrostatically-driven crosslinking of the cCNF and LNPs. A similar observation was also observed by Qu et al. (2021) on the crosslinking of nanocellulose using calcium chloride. Further addition of LNPs decreased G, indicating that there is a threshold of the amount of LNPs that can promote gelling, but detailed work to explain this phenomenon is beyond the scope of the present study. For the cLNP/TCNF combination, only a slight increase in G′ was observed. The effect of crosslinking in the viscoelastic properties of gel seemed to be more dominant in nanocellulose containing short fibrils than in those with longer fibrils.

3.2. Cryogels and their physico-mechanical properties

The cryogels have an entangled network of cellulose nanofibrils as the skeletal framework, where the LNPs are anchored by electrostatic attraction. For the TCNF-cLNP cryogels, the electrostatic attraction is between the negative carboxyl groups of TCNF at carbon-6 and the cationic ternary ammonium groups attached to the cLNPs. The electrostatic attraction between the cationic groups in cCNF and anionic carboxyls of the LNPs served as the anchoring mechanism of the LNPs to the cCNF.

The physical appearance, morphology and physico-mechanical properties of the prepared cryogels are presented in Fig. 2. The LNP/cLNP-decorated nanocellulose cryogels were brown, and darker with increasing lignin content (Fig. S2). The cryogels were macroporous and showed layered sheets, randomly coated with spherical LNPs or cLNPs (Fig. 2A and B & S2). A sheet-like cellulosic network with large pores of several micrometers induced by the growing ice crystals during freezing is typically observed for cellulosic cryogels (Buchtová and Budtova, 2016).

The bulk density of the cryogels increased because of the addition of lignin since the solid content increased without significant increase in the volume of the cryogels. The TCNF-based cryogels, which showed shrinkage during drying, however, had higher bulk density than the cCNF-based ones. The obtained bulk density values ranging from 9 to 16 mg/cm^3 and 7–10 mg/cm^3 for the TCNF- and cCNF-based cryogels, respectively, fall within those reported in the literature for nanocellulose-based porous materials produced by freeze drying (Chen et al., 2021).

The firmness, which is defined here as the force required to compress to 50% of the original height also increased with increasing lignin content both for the cCNF- and TCNF-based cryogels. These results highlighted the function of LNPs and cLNPs as crosslinking agents that improved the resistance of the nanocellulose-based cryogels towards

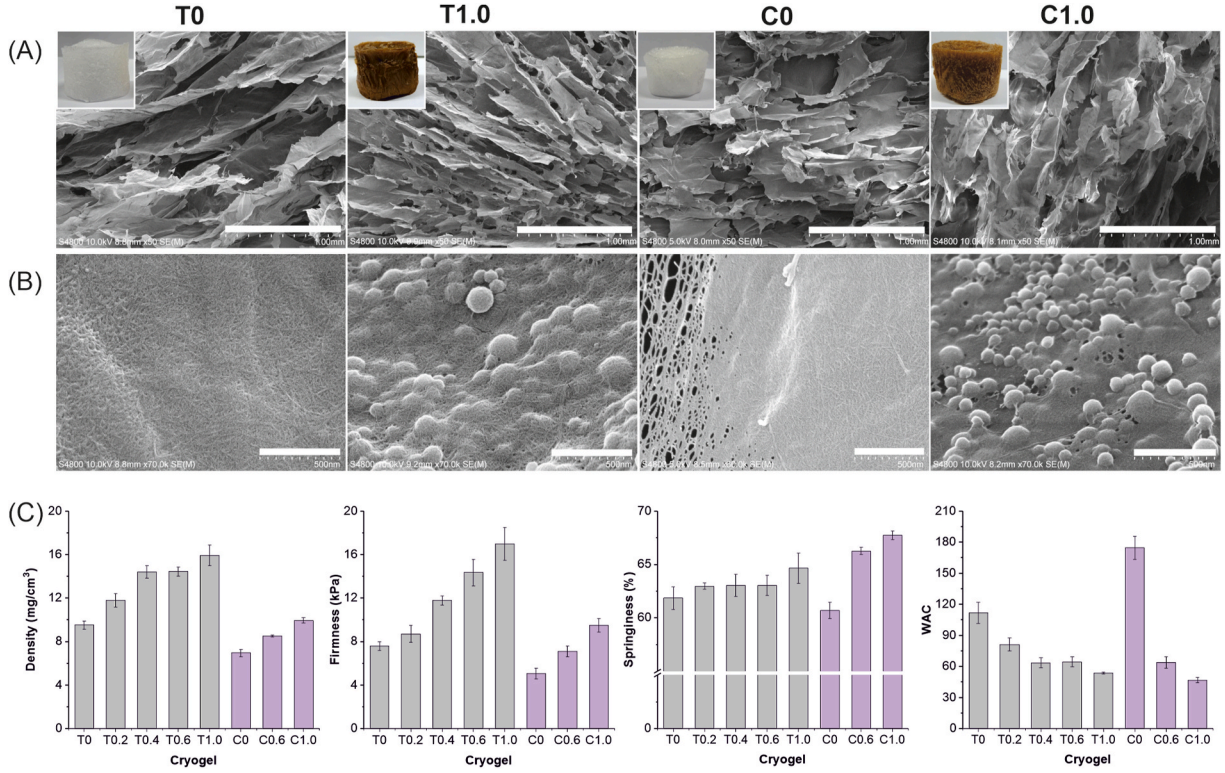

Fig. 2. Appearance (insets) and FESEM images (A&B) and physico-mechanical properties, including density, firmness, springiness and water absorption capacity (WAC) (C) of the nanocellulose-based cryogels with varying LNP or cLNP content. Scale bars in (A) and (B) correspond to 1 mm and 500 nm, respectively. Error bars in (C) are ± standard error of the mean of at least five measurements.

compressive deformation. Similar findings in previous work also revealed the improvement in compressive strength of crosslinked nanocellulosic porous materials (Hossain et al., 2021; Zhu et al., 2019).

The springiness, measured by the percentage of which the cryogel returned to its original height after releasing the applied compressive force remained almost the same for TCNF-based cryogels but increased for cCNF-based cryogels with increasing LNP content. The recovery after compression ranged from 61 to 64% and 60–67% for TCNF- and cCNF-based cryogels, respectively.

The WAC decreased by the addition of LNPs or cLNPs, which are known to be less hygroscopic than the nanocelluloses. The addition of cLNPs to TCNF or LNPs to cCNF at 1:1 ratio reduced the WAC by 44% and 60%, respectively. This decrease in WAC further affirmed the crosslinking brought by the LNPs or cLNPs, similar to that observed by Hossain et al. (2021) in the water absorption capacity of nanocelluloses crosslinked by polyethyleneimine or hexamethylenediamine.

3.3. The adsorption capacity and surface charge

The initial assessment of the adsorption potential of the LNP/cLNP-decorated nanocellulose cryogels was achieved by determining the adsorption capacity, *q*, which refers to the amount of adsorbed materials (mg) per unit mass (g) of the adsorbent. It is calculated from the equation

$$q = \frac{(C_O - C_f)\, V}{m} \quad (1)$$

where C_O and C_f are the initial and final concentration (mg/L), respectively, V is the volume (L) of the solution, and m is the dry mass in grams of the adsorbent. The C_O was based on the results of the blank analysis. The determination of q was done in a multi-component system, where six different pharmaceuticals were all dissolved in the solution. The selected pharmaceuticals were of varying polarity, aromaticity and ionizability in water. These include the polar aromatic neutral acetaminophen (ACE), the non-polar aromatic neutral carbamazepine (CBZ), the anionic aromatic diclofenac (DCF) and ibuprofen (IBU), the highly polar aliphatic cationic MTF, and the cationic aromatic MPL and TRA. This selection enables assessment of the selectivity of the cryogels towards a specific group alongside the efficiency to adsorb simultaneously different types of pharmaceuticals.

Fig. 3 shows the q values of each cryogel for different APIs and the absolute values of the surface charge density of each cryogel. The surface charge density showed a decreasing trend with an increasing ratio of lignin content because of charge neutralization. The net surface charge of the TCNF- and cCNF-based cryogels were negative and positive, respectively. It is evident from the q values that the overall surface charge defined the type of APIs strongly adsorbed by the cryogels. The anionic TCNF-based cryogels were highly selective for the positively charged MTF, MPL and TRA than for the negatively charged IBU and DCF, or the neutral ACE and CBZ (Fig. 3a). Similarly, the cationic cCNF-based cryogels adsorbed anionic IBU and DCF more than the cationic or neutral ones (Fig. 3b). These results exemplify the significant contribution of electrostatic attractive force in the adsorption potential of the cryogels.

Other types of interactive forces such as hydrophobic or π-π aromatic ring interactions seemed to play a role with the addition of cLNPs to TCNF. This is evident from the increasing q values for MPL and TRA with increasing cLNP content. At a cLNP/TCNF ratio of 0.6 or higher, the q values for MPL and TRA were significantly higher (50%) than those without cLNP (T0), despite the decrease in the net negative surface charge. This improvement can be attributed to the possible π-π aromatic ring interactions between these aromatic cationic APIs and cLNPs. This assumption is further supported by the lack of improvement in the q value of T0.6 and T1.0 for the highly polar aliphatic cationic MTF. The finding was consistent with our earlier report on the capacity of cLNPs to remove aromatic cationic pharmaceuticals but not aliphatic cationic ones, like the MTF (Agustin et al., 2022). However, the aromatic ring interaction was not able to enhance the removal of the aromatic ACE, CBZ, DCF and IBU. The anchorage of the ternary ammonium cations in cLNPs to the TCNF removed the capacity of cLNPs to adsorb aromatic pharmaceuticals that are anionic or neutral. It is possible that the repulsive force between the anionic pharmaceuticals and the negative surface of the TCNF-based cryogels was too strong to be overcome by other modes of interaction. Overall, the addition of cLNPs to TCNF-based cryogels resulted in an enhanced selectivity towards cationic aromatic pharmaceuticals.

Adsorption other than that driven by electrostatic forces was also observed in cCNF-based cryogels containing LNPs. Despite the decrease in the positive surface charge of the cCNF-based cryogels with the addition of LNPs, the adsorption for the anionic aromatic DCF significantly increased at 0.6 LNP to cCNF ratio (Fig. 3b). However, this behavior was not observed for the other anionic aromatic IBU, which

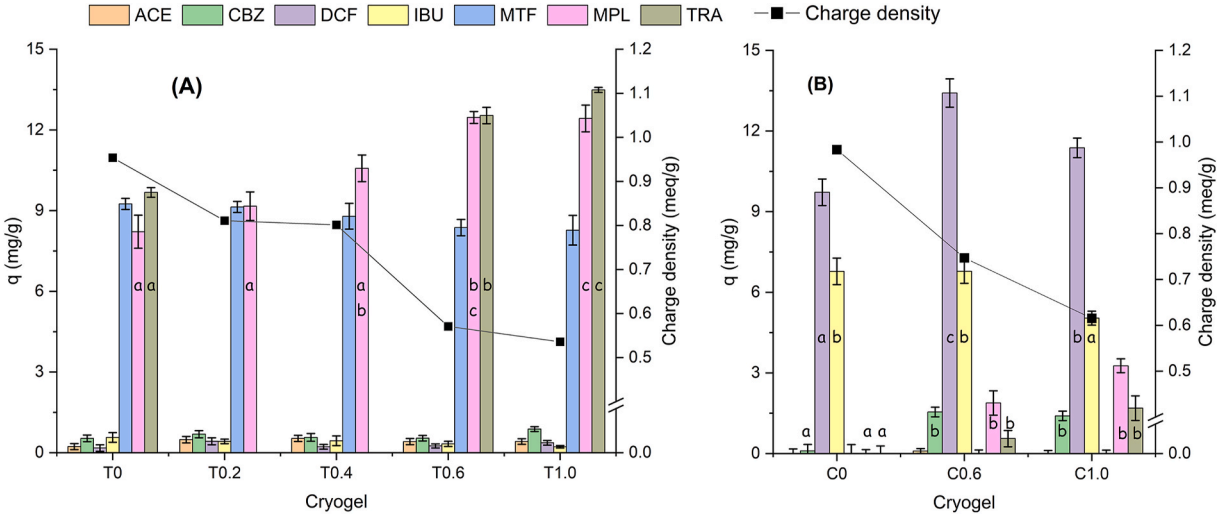

Fig. 3. The adsorption capacity (q) of TCNF- (a) and cCNF-based (b) cryogels decorated with varying ratios of cLNPs and LNPs, respectively, for different types of pharmaceuticals plotted against surface charge density. Adsorption conditions: multi-component, room temperature, 1.5 h, 20 mg/L initial concentration of each pharmaceutical, 1 mg/mL mass to volume ratio of cryogel to pharmaceutical solution, pH ≈ 6. Bars with different lowercase letters represent means with significant differences ($p < 0.05$). Error bars represent ± standard error of the mean of at least five measurements.

could be due to its lower aromaticity than the DCF. Unlike the addition of cLNP to TCNF, the incorporation of LNPs to cCNF improved the adsorption of the cationic MPL and TRA, and of the neutral CBZ, possibly induced by aromatic ring interaction or electrostatic interactions brought by free carboxyl groups of the LNPs. These findings suggest that anchoring LNPs to cCNF promotes the removal of a wider range of pharmaceuticals than anchoring cLNPs to an anionic TCNF. When LNPs are anchored to a cationic substrate, it is the carboxyl groups of the lignin that are consumed to electrostatically bind with the cCNF, possibly leaving the phenolic groups more labile and active or leaving some carboxyl groups free. On the other hand, in the cLNPs, the phenolic groups carry the cationic groups, which eventually formed electrostatic attraction with the TCNF. This possibly rendered the phenolic groups to be less available for interaction, hindering the cCNF/TCNF cryogels to adsorb anionic or neutral aromatic APIs.

3.4. Effect of pH

The pH of the surrounding medium affects both the adsorbent and the adsorbate, having pH-dependent ionizable groups, such as carboxyls, hydroxyls and amine groups. The protonation or deprotonation of these groups influences the charge of both the adsorbent and adsorbate, thus affecting the adsorption process. Fig. 4A and B shows the effect of pH on the adsorption capacity of T0.6 and C0.6 cryogels, respectively, which were selected because these cryogels already displayed significantly different adsorption behavior in comparison to pure nanocellulose. Choosing these cryogels over T1.0 or C1.0 saves the amount of LNPs or cLNPs added to the cryogels. Only pH 3 and 6 were tested because our previous study showed that the adsorption behavior of different types of LNPs and nanocelluloses revealed large differences between pH 3 and 5 and only slight differences between pH 5 and 8.5 (Agustin et al., 2022). However, instead of using pH 5, pH 6 was chosen to ensure that the carboxyl (pKa ~5) is mostly in the deprotonated form. Moreover, the fraction of ionized forms of the pharmaceuticals between pH 6 and 8.5 were not significantly different (Fig. S3). A pH greater than 8.5 was not tested because LNPs starts to dissolve at pH 9 as observed in our previous work.

For the anionic T0.6 cryogel, q increased for the neutral CBZ and anionic IBU at pH 3, however, it was at the expense of a significant reduction in q for the cationic MPL and MTF. At pH 3, both the T0.6 cryogel and IBU (pKa = 4.9) are expected to have less anionic character because of the protonation of the carboxyl groups (pKã5). This possibly weakens the electrostatic repulsion enabling the improvement in the adsorption for IBU and CBZ (pKa = 14) via aromatic ring interactions. However, the protonation of the carboxyl in T0.6 is expected to decrease the anionic surface charge density, thereby weakening the interaction with the cationic MPL (pKa = 9.6) and MTF (pKa = 12). The aromatic, highly polar and neutral ACE (pKa = 9.4), consistently showed weak affinity towards the cryogel at both pH.

The cationic C0.6 cryogel displayed a decrease in q for all pharmaceuticals at pH 3 except for CBZ, which was not significantly affected by the change in pH. At pH 3, the ternary ammonium groups in C0.6 remain positive and the free carboxyl groups of LNPs were protonated. An increase in cationic character of the C0.6 cryogels at pH 3 is expected. However, this did not result in the improvement of the removal of the anionic IBU because at this pH, the IBU (pKa = 4.9) was also protonated. Despite this, aromatic ring interaction, hydrogen bonding or hydrophobic interactions could drive the weak removal of IBU at pH 3. The adsorption of MPL (pKa = 9.4) was favored at pH 6 where the unbound carboxyl groups (pKa ~5) of LNPs were ionized. The lack of affinity of MPL towards the C0.6 cryogel at pH 3 is possibly due to the dominant repulsive force, because both were cationic. At both pH, the highly polar ACE and MTF remained difficult to remove by the C0.6 cryogel.

Despite the slight improvement in the removal of some pharmaceuticals at pH 3, both cryogels were more effective at pH 6. For both cryogels and at both pH, the neutral and highly polar ACE was consistently difficult to remove. The comparison of the adsorption of DCF (pKa = 4.2) was not shown because at pH 3, DCF is mostly in the protonated form, which precipitated out in the solution. This is also shown by the disappearance of the DCF peak in the chromatogram at pH 3.

3.5. Effect of morphology

The behavior of materials is defined not only by their chemical structure but also by their morphology. Thus, the effect of the morphology of the lignin nanomaterial towards the adsorption behavior of the cryogels was investigated. It answers the question of whether there is a need to prepare lignin as spherical nanoparticles or use other forms of lignin. For this purpose, cryogels with the same 0.6:1 lignin to nanocellulose mass ratio were prepared using non-spherical lignin. The soluble cationic lignin was combined with TCNF producing the T0.6 L cryogel. The LNPs produced by ultrasonication (Agustin et al., 2019) and with drying did not produce spherical particles were combined with cCNF yielding the C0.6 L cryogel. As shown in Fig. 5, the morphology of the lignin nanomaterials affected the surface properties (Fig. 5A) and adsorption behavior (Fig. 5B) of the cryogels. The T0.6 L had

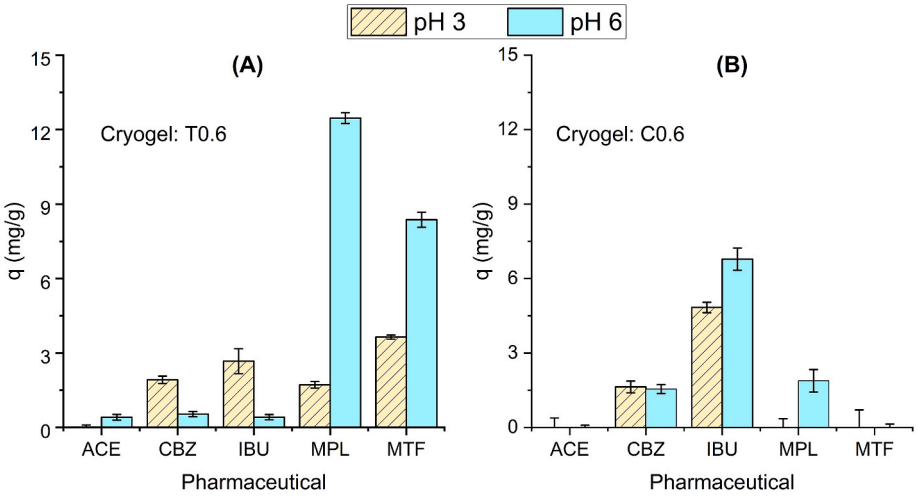

Fig. 4. The effect of pH on the adsorption capacity,q, towards different pharmaceuticals of the nanocellulose cryogels decorated with spherical LNPs (T0.6) and cLNPs (C0.6). Adsorption conditions: multi-component, room temperature, 1.5 h, 20 mg/L initial concentration of each pharmaceutical, 1 mg/mL mass to volume ratio of cryogel to pharmaceutical solution.

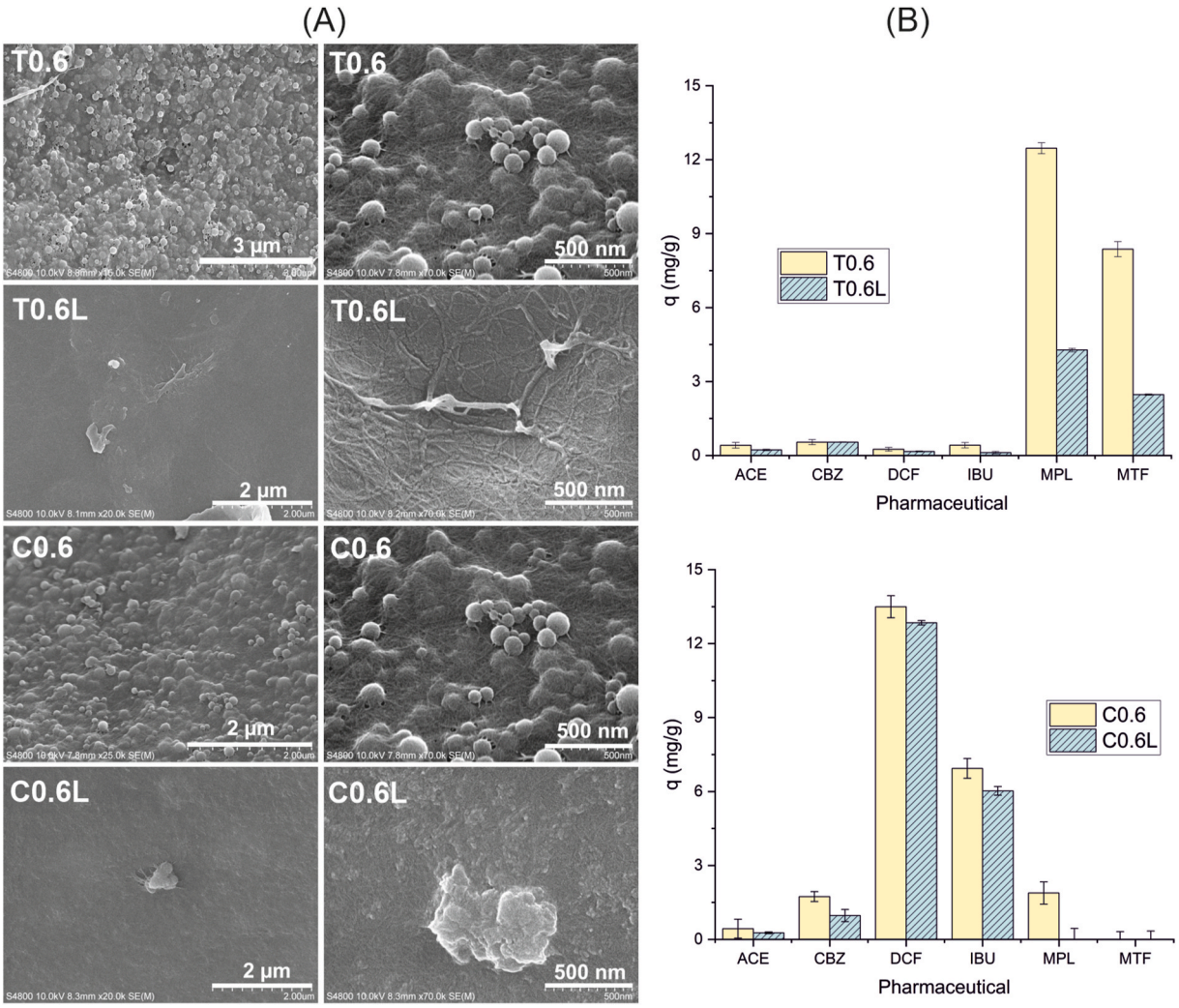

Fig. 5. The surface morphology (A) and adsorption capacity,q, towards different pharmaceuticals (B) of the nanocellulose cryogels decorated with spherical LNPs (T0.6) and cLNPs (C0.6), and non-spherical anionic (T0.6 L) and cationic (C0.6 L) lignin forms, at a lignin to nanocellulose ratio of 0.6:1. Error bars represent ± standard error of the mean of at least three replicates. Adsorption conditions: multi-component, room temperature, 1.5 h, 20 mg/L initial concentration of each pharmaceutical, 1 mg/mL mass to volume ratio of cryogel to pharmaceutical solution, pH ≈ 6.

significantly lower q for the cationic MPL and MTF than those of the T0.6. If compared with the q values of T0 presented in Fig. 3, those of the T0.6 L were even lower suggesting a lack of improvement in q when the soluble cationic lignin is used. Similarly, the C0.6 L showed lower q values for all the pharmaceuticals than the C0.6. The results suggest that the spherical lignin nanomaterials rendered higher adsorption efficiency than using the soluble or irregularly shaped forms of lignin. As seen in Fig. 5A, the surface of the cryogels was much smoother than when it is decorated with spherical LNPs or cLNPs. The smoothness is much more pronounced in the T0.6 L because the soluble cationic lignin seemed to coat the TCNF uniformly, unlike the spherical cLNPs that are anchored randomly creating a rough surface. The C0.6 L also showed a smoother surface than the C0.6 but with agglomerated lignin. It is possible that with spherical lignin nanomaterials, the increase in roughness resulted in a higher surface area of lignin available for interaction with the pharmaceuticals. This phenomenon is similar to the findings of Hsieh et al., (2005), where the increase in surface area of the titanium oxide nanoparticle-coated polymer was linked to increasing roughness with increasing amount of titanium oxide. Moreover, the three-dimensional spheres possibly allowed some of the active functionalities of lignin to be oriented on the surface and available for adsorption. With the soluble or non-spherical forms that were flexible, most of their active groups were possibly bonded to the nanocellulose.

3.6. Adsorption isotherms

To determine the maximum adsorption capacity (q_m), single-analyte adsorption experiments were conducted for T0.6 and C0.6 cryogels. Only the pharmaceuticals that showed significant improvement in q relative to the non-lignin containing cryogels were investigated. These were the MPL and TRA for T0.6 and DCF for C0.6 cryogels. The initial concentrations were varied and the values of equilibrium adsorption capacity (q_e) were plotted against equilibrium concentrations (C_e). Non-linear adsorption isotherm models, which include the Freundlich, Langmuir, and Sips models were used in fitting the experimental data using the Origin Lab.

The Freundlich isotherm assumes multilayer adsorption on heterogeneous surfaces and has a nonlinear form shown in equation (2) (Al-Ghouti and Da'ana, 2020; Freundlich, 1906; Wang and Guo, 2020)

$$q_e = K_F C_e^{1/n_F} \quad (2)$$

where K_F and n_F are constants related to adsorption capacity and heterogeneity factor from the adsorption sites, respectively. The ratio $1/n_F$ indicates the irreversibility ($1/n_F = 0$), favorability ($0 < 1/n_F < 1$), or unfavorability ($1/n_F > 1$) of the adsorption process (Al-Ghouti and Da'ana, 2020; Freundlich, 1906; Wang and Guo, 2020).

The Langmuir isotherm is a semi-empirical model represented by the nonlinear equation (3) (Langmuir, 1918)

$$q_e = \frac{q_m K_L C_e}{1 + K_L C_e} \quad (3)$$

where K_L represents the equilibrium constant. This isotherm assumes monolayer adsorption, i.e. if a molecule is adsorbed onto a particular site, no other molecules can be adsorbed on the same site at the same time (Langmuir, 1918; Rajahmundry et al., 2021). Langmuir isotherm model predicts adsorption on a homogeneous surface with constant energy of adsorption and negligible interaction between adsorbate molecules (Wang and Guo, 2020).

The Sips isotherm is a hybrid model obtained by combining Freundlich and Langmuir isotherms and can describe adsorption on homogeneous or heterogeneous systems. The nonlinear form of the Sips isotherm is given by equation (4)

$$q_e = \frac{q_m K_s C_e^{n_s}}{1 + K_s C_e^{n_s}} \quad (4)$$

where K_S is the Sips equilibrium constant and n_S describes the Sips heterogeneity factor (Mozaffari Majd et al., 2022; Sips, 1948). When $n_S = 1$, the Sips model becomes a Langmuir equation indicating homogeneous adsorption system. At low adsorbate concentrations and low K_S, the Sips model favors the Freundlich model (Mozaffari Majd et al., 2022; Sips, 1948; Wang and Guo, 2020).

Fig. 6 shows the fitting of different isotherm models to the experimental adsorption data. The isotherm parameters are summarized in Table S2, and based on the values of the coefficient of determination (R^2) and reduced chi-square, the Sips isotherm model gave the best fit for the three pharmaceuticals. The heterogeneity factor, n_S, was less than unity, an indication of heterogeneous adsorption system. The calculated q_m of C0.6 for DCF was 350 mg/g and found to be lower than most nanocellulose-base adsorbents functionalized by various chemical modification techniques (Table 1) but higher than those of the polyethyleneimine- or polypyrrole-treated cellulose-based adsorbents. The $q_m$of T0.6 for MPL and TRA were 91 and 150 mg/g, respectively. MPL and TRA removal by adsorption was less studied than the DCF and this current work was the first to utilize nanocellulose-based adsorbents, thus the q_m values were compared with other types of adsorbents available in literature. The T0.6 cryogel was much inferior to spirulina-derived carbon but only slightly less to carrageenan-based adsorbent in adsorbing MPL. With TRA, T0.6 was comparable to those of smectite clay mineral or NaOH-treated algal biomass. However, it should be noted that comparisons on the feasibility of the materials at this early stage of testing as adsorbents does not guarantee similar performances if adsorption experiments were all performed at different conditions.

3.7. Reusability

In the development of new adsorbents, reusability is a huge concern. Reusability covers the ease of regenerating the adsorbent, i.e. desorbing the adsorbate, and the capacity of the adsorbent to maintain its efficiency with several uses. Expensive production costs are often compensated if the adsorbents are reusable.

The key characteristic required for an adsorbent to be reusable is its durability or stability with repeated and prolonged exposure to the medium of adsorption. Thus, an initial assessment of the durability of the nanocellulose-based cryogels in water was performed qualitatively. The cryogels were soaked in water, taken out and pressed (Fig. S4). The cCNF-based cryogels disintegrated easily after 4 h of soaking in water. Even without pressing, C0 already showed signs of structural collapse. The crosslinking brought by LNPs strengthened the structure, enabling the C0.6 cryogel to maintain its form when wetted, but was not sufficient to resist disintegration when pressed. The TCNF-based cryogels were resistant to disintegration in water, and were further strengthened by the addition of cLNPs. The T0.6 cryogel kept its structural integrity with prolonged and repeated exposure to water. Upon compression in the wet state, it did not disintegrate, and it was possible to lift, press and soak again in water, returning to its original shape (Fig. 7A). Even after five cycles of adsorption-desorption experiment, the T0.6 cryogel was intact and the surface was still randomly coated with cLNPs.

The reusability of the T0.6 cryogel was then tested with MPL as the model API, since MPL was significantly adsorbed by T0.6. The desorption of MPL was effective in a slightly acidic solution, either with shaking or sonication, which desorbed more than 90% of the adsorbed MPL (Fig. 7B). In acidic medium, the carboxyl groups that hold the MPL become protonated, thereby releasing the adsorbed MPL. Five cycles of adsorption-desorption experiments were then performed using the acidic media with shaking mode as the desorption method. The removal efficiency of the T0.6 cryogel for MPL reached as high as 85% in the first cycle and slightly decreased in the second cycle. At the third cycle, the removal efficiency significantly decreased to about 60% and remained almost the same until the fifth cycle (Fig. 7C). A similar removal efficiency, which did not decrease below 60% after 5 cycles of adsorption-desorption experiment, was also observed in the polyvinylamine- and reduced graphene oxide-modified nanocellulose adsorbents, but for the removal of another type of drug, DCF.

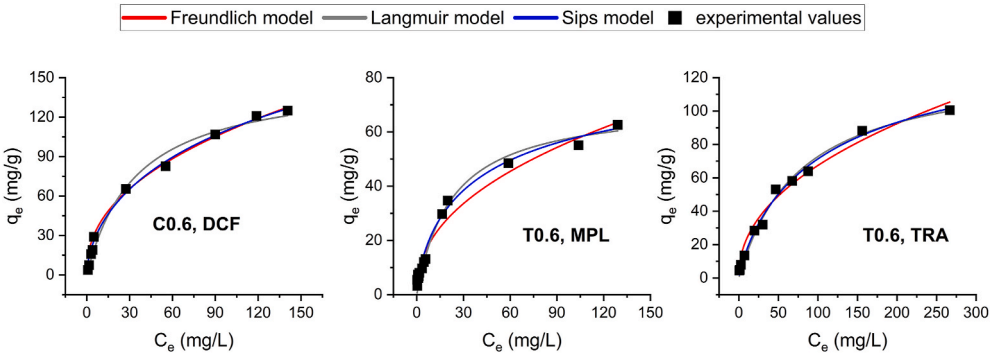

Fig. 6. The fitting of different adsorption isotherm models to the plot of experimental values of equilibrium concentrations (C_e) versus equilibrium adsorption capacity (q_e). Adsorption conditions: single-component, room temperature, 2.5 h, 1 mg/mL mass to volume ratio of cryogel to pharmaceutical solution, pH ≈ 6.

Table 1
Comparisons between the adsorption potential of the developed nanocellulose-based cryogels to those available in literature.

Pharmaceutical	Adsorbent	pH	Temperature	Isotherm	q_m (mg/g)	Reference
Diclofenac	Cellulose nanocrystalline modified with polyvinylamine and reduced graphene oxide	7	25	Langmuir	606	Lv et al. (2021)
	Nanocellulose fine-tuned poly (acrylic acid) hydrogel	Unadjusted	25	Langmuir	560	Tie et al. (2022)
	Nanocellulose grafted with 1,3,5-Tris (4-aminophenyl)benzene and trimesoyl chloride	7	25	Langmuir	526	Liu et al. (2022)
	Bilayer ethylenediamine-functionalized cellulose nanocrystals/chitosan composite	4.5	25	Langmuir	444	Hu et al. (2019)
	LNP-decorated cCNF cryogel	6	Ambient	Sips	350	This study
	Polyethyleneimine-modified cellulose aerogels	5	25	Langmuir	294	Chen et al. (2022)
	Polypyrrole treated cellulose fiber	6	Ambient	Dual-site Langmuir-Freundlich	210	Pires et al. (2017)
Metoprolol	Spirulina-based carbon	5	25	Sips	661	Pedrosa et al. (2022)
	Glutaraldehyde cross-linked carrageenan microparticles	6	20	Sips	109	Nanaki et al. (2015)
	cLNP-decorated TCNF cryogel	6	Ambient	Sips	91	This study
Tramadol	Sodium smectite clay mineral	7–7.5	20	Langmuir	210[a]	Thiebault et al. (2015)
	cLNP-decorated TCNF cryogel	6	Ambient	Sips	150	This study
	NaOH treated algal biomass (Scenedesmus obliquus)	NA	Ambient	Langmuir	140	Ali et al. (2018)

[a] Value in the reference was converted from mole/g to mg/g.

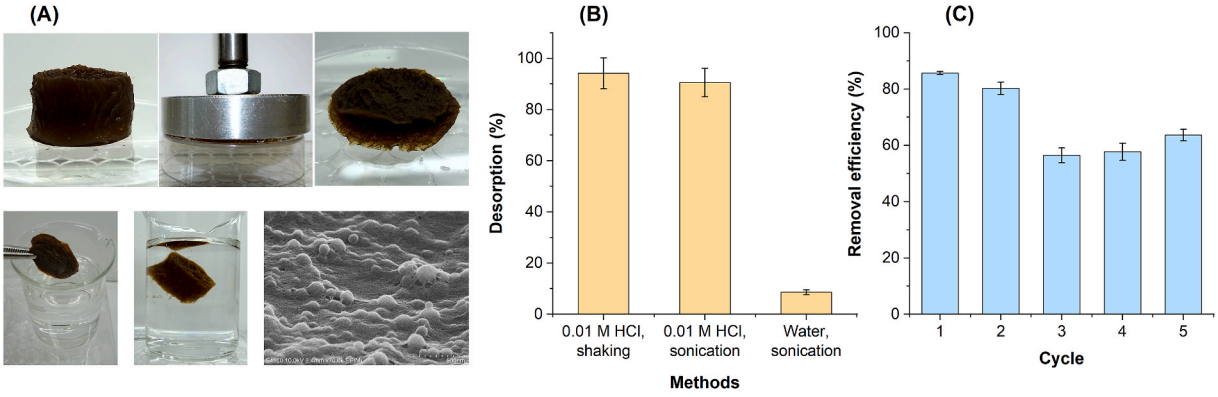

Fig. 7. The wet T0.6 cryogel that keeps its structural integrity after repeated soaking and compression and its FESEM micrograph after 5 cycles of adsorption-desorption (a), the comparison of different modes of desorbing metoprolol after adsorption (b) and the removal efficiency of T0.6 cryogel for five cycles of adsorption-desorption experiments with metoprolol (c). Error bars represent ± standard error of the mean of at least three measurements.

4. Conclusions and future outlook

The feasibility of adsorption in mitigating the impacts of pharmaceutical pollution relies on the development of reusable adsorbents with high affinity towards various types of pharmaceuticals. With the aim of developing such adsorbents, different types of LNPs and nanocelluloses were combined to prepare nanocellulose-based cryogels as adsorbents for pharmaceuticals in a multi-component adsorption system. The pharmaceuticals were carefully selected such that they encompass a wide range of chemical variability to assess the selectivity and efficiency of the cryogels during simultaneous adsorption.

The LNPs act as functionalizing agents, and the type (cationic or unmodified), amount and morphology of the LNPs anchored to the nanocellulose affect their adsorption potential towards different pharmaceuticals. Anchoring cLNPs to TCNF only improved the capacity of TCNF to adsorb cationic aromatic pharmaceuticals such as TRA and MPL. The cLNPs had no significant effect in adsorbing other types of pharmaceuticals (aromatic anionic, aromatic neutral, or aliphatic cationic). Anchoring unmodified LNPs to cCNF widened the adsorption potential of the cCNF-based cryogels resulting in improved removal of cationic, anionic and neutral aromatic pharmaceuticals. However, to achieve such improvement in adsorption potential, the ratio of LNPs or cLNPs to nanocellulose must be higher than 0.6:1 and spherical lignin nanomaterials must be used.

The LNPs also act as crosslinking agents. The crosslinking between the nanofibrils aided by electrostatic attraction improved the firmness and decreased the water absorption of the cryogels. More importantly, the crosslinking enhanced the resistance of the cryogels towards disintegration with repeated exposure to water, enabling the reusability of the cryogels. However, the extent of improvement brought by crosslinking depends also on the nanofibril length, thus it is important to consider the aspect ratio of the starting nanocellulose in order to achieve sufficient stability with repeated exposure in water.

Overall, the study highlighted the challenges in developing reusable nanostructured wood-based adsorbents that can remove a wide array of pharmaceuticals. Several aspects were taken into account but some limitations are worth considering for future investigations. For instance, the concentration of pharmaceuticals in this study was way higher than those found in real wastewaters, and the removal efficiency could be different at very low concentrations. Furthermore, increasing the surface area by using different drying techniques, such as supercritical drying, would be worth exploring. Aside from pH, other adsorption parameters, such as temperature or adsorbent dosage, could be varied to study the adsorption kinetics.

While there were limitations, the most important finding this study revealed is the greater potential of unmodified LNPs than cLNPs in expanding the adsorption potential of the nanocellulose cryogels. This implies that designing bio-based adsorbents without further chemical modification is feasible if the LNPs are paired with naturally occurring cationic polymeric matrices such as chitin. This paves the way for creating greener and more sustainable adsorbents.

Credit author statement

M.Agustin: Conceptualization, Formal analysis, Funding acquisition, Investigation, Methodology, Writing – original draft writing. M.Lehtonen: Conceptualization, Methodology, reviewing and editing. M. Kemell: Resources, Methodology, reviewing and editing. E.Oliaei: Resources, Methodology, reviewing and editing. P. Lahtinen: Resources, Methodology, reviewing and editing. K.S. Mikkonen: Conceptualization, Resources, reviewing and editing, Supervision.

Declaration of competing interest

The authors declare that they have no known competing financial interests or personal relationships that could have appeared to influence the work reported in this paper.

Data availability

Data will be made available on request.

Acknowledgments

MBA thanks the Academy of Finland (Grant number 330617) for funding. Troy Faithfull is thanked for his help in polishing the manuscript. The ALD center Finland research infrastructure is acknowledged for the FESEM imaging.

Appendix A. Supplementary data

Supplementary data to this article can be found online at https://doi.org/10.1016/j.jenvman.2022.117210.

References

Agustin, M.B., Mikkonen, K.S., Kemell, M., Lahtinen, P., Lehtonen, M., 2022. Systematic investigation of the adsorption potential of lignin- and cellulose-based nanomaterials towards pharmaceuticals. Environ. Sci. Nano 9, 2006–2019. https://doi.org/10.1039/d2en00186a.

Agustin, M.B., Penttilä, P.A., Lahtinen, M., Mikkonen, K.S., 2019. Rapid and direct preparation of lignin nanoparticles from alkaline pulping liquor by mild ultrasonication. ACS Sustain. Chem. Eng. 7, 19925–19934. https://doi.org/10.1021/acssuschemeng.9b05445.

Ahmed, M., Mavukkandy, M.O., Giwa, A., Elektorowicz, M., Katsou, E., Khelifi, O., Naddeo, V., Hasan, S.W., 2022. Recent developments in hazardous pollutants removal from wastewater and water reuse within a circular economy. npj Clean Water 5, 1–25. https://doi.org/10.1038/s41545-022-00154-5.

Al-Ghouti, M.A., Da'ana, D.A., 2020. Guidelines for the use and interpretation of adsorption isotherm models: a review. J. Hazard Mater. 393, 122383 https://doi.org/10.1016/j.jhazmat.2020.122383.

Ali, M.E.M., Abd El-Aty, A.M., Badawy, M.I., Ali, R.K., 2018. Removal of pharmaceutical pollutants from synthetic wastewater using chemically modified biomass of green alga Scenedesmus obliquus. Ecotoxicol. Environ. Saf. 151, 144–152. https://doi.org/10.1016/j.ecoenv.2018.01.012.

Aoudi, B., Boluk, Y., Gamal El-Din, M., 2022. Recent advances and future perspective on nanocellulose-based materials in diverse water treatment applications. Sci. Total Environ. 843, 156903 https://doi.org/10.1016/j.scitotenv.2022.156903.

Bhagwat, V.R., 2019. Safety of water used in food production. Food Saf. Hum. Heal. 219–247. https://doi.org/10.1016/B978-0-12-816333-7.00009-6.

BIO Intelligence Service, 2013. Study on the Environmental Risks of Medicinal Products. Final Report prepared for Executive Agency for Health and Consumers.

Buchtová, N., Budtova, T., 2016. Cellulose aero-, cryo- and xerogels: towards understanding of morphology control. Cellulose 23, 2585–2595. https://doi.org/10.1007/s10570-016-0960-8.

Buchtová, N., Pradille, C., Bouvard, J.-L., Budtova, T., 2019. Mechanical properties of cellulose aerogels and cryogels. Soft Matter 7901–7908. https://doi.org/10.1039/c9sm01028a.

Chen, M., Yang, G., Liu, Y., Lv, Y., Sun, S., Liu, M., 2022. Preparation of amino-modified cellulose aerogels and adsorption on typical diclofenac sodium contaminant. Environ. Sci. Pollut. Res. 29, 19790–19802. https://doi.org/10.1007/s11356-021-17214-x.

Chen, Y., Zhang, L., Yang, Y., Pang, B., Xu, W., Duan, G., Jiang, S., Zhang, K., 2021. Recent progress on nanocellulose aerogels: preparation, modification, composite fabrication, applications. Adv. Mater. 33 https://doi.org/10.1002/adma.202005569.

Crini, G., Lichtfouse, E., Wilson, L.D., Morin, N., 2019. Conventional and non - conventional adsorbents for wastewater treatment. Environ. Chem. Lett. 17, 195–213. https://doi.org/10.1007/s10311-018-0786-8.

De Andrade, J.R., Oliveira, M.F., Da Silva, M.G.C., Vieira, M.G.A., 2018. Adsorption of pharmaceuticals from water and wastewater using nonconventional low-cost materials: a review. Ind. Eng. Chem. Res. 57, 3103–3127. https://doi.org/10.1021/acs.iecr.7b05137.

Dusi, E., Rybicki, M., Jungmann, D., 2019. The Database "Pharmaceuticals in the Environment" - Update and New Analysis: Final Report. German Environmental Agency, Dresden.

Ebele, A.J., Abou-Elwafa Abdallah, M., Harrad, S., 2017. Pharmaceuticals and personal care products (PPCPs) in the freshwater aquatic environment. Emerg. Contam. 3, 1–16. https://doi.org/10.1016/j.emcon.2016.12.004.

Eichhorn, S.J., Etale, A., Wang, J., Berglund, L.A., Li, Y., Cai, Y., Chen, C., Cranston, E.D., Johns, M.A., Fang, Z., Li, G., Hu, L., Khandelwal, M., Lee, K.Y., Oksman, K., Pinitsoontorn, S., Quero, F., Sebastian, A., Titirici, M.M., Xu, Z., Vignolini, S., Frka-Petesic, B., 2022. Current international research into cellulose as a functional nanomaterial for advanced applications. J. Mater. Sci. 57, 5697–5767. https://doi.org/10.1007/s10853-022-06903-8.

European Commission, 2022. Commission implementing decision (EU) 2022/1307. Off. J. Eur. Union [WWW Document]. https://eur-lex.europa.eu/legal-content/EN/TXT/?uri=CELEX%3A32022D1307&qid=1658824912292.

Farooq, M., Zou, T., Riviere, G., Sipponen, M.H., Österberg, M., 2019. Strong, ductile, and waterproof cellulose nanofibril composite films with colloidal lignin particles. Biomacromolecules 20, 693–704. https://doi.org/10.1021/acs.biomac.8b01364.

Figueiredo, P., Lahtinen, M.H., Agustin, M.B., Carvalho, M. De, Hirvonen, S., Penttilä, P. A., Mikkonen, K.S., 2021. Green Fabrication Approaches of Lignin Nanoparticles from Different Technical Lignins : A Comparison Study, pp. 1–14. https://doi.org/10.1002/cssc.202101356.

Freundlich, H.M.F., 1906. Over the adsorption in solution. J. Phys. Chem. 57, 385–471.

Herrera, M., Thitiwutthisakul, K., Yang, X., Rujitanaroj, P., Rojas, R., Berglund, L., 2018. Preparation and evaluation of high-lignin content cellulose nanofibrils from eucalyptus pulp. Cellulose 25, 3121–3133. https://doi.org/10.1007/s10570-018-1764-9.

Hossain, L., Raghuwanshi, V.S., Tanner, J., Garnier, G., 2021. Modulating nanocellulose hydrogels and cryogels strength by crosslinking and blending. Colloids Surfaces A Physicochem. Eng. Asp. 630, 127608 https://doi.org/10.1016/j.colsurfa.2021.127608.

Hsieh, C.-T., Chen, J.-M., Kuo, R.-R., Lin, T.-S. Wu, C-F., 2005. Influence of surface roughness on water-and oil-repellent surfaces coated with nanoparticles. Appl. Surf. Sci. 240 (1–4), 318–326.doi.org/10.1016/j.colsurfa.2022.128570.

Hu, D., huang, H., Jiang, R., Wang, N., Xu, H., Wang, Y.G., Ouyang, X. kun, 2019. Adsorption of diclofenac sodium on bilayer amino-functionalized cellulose nanocrystals/chitosan composite. J. Hazard Mater. 369, 483–493. https://doi.org/10.1016/j.jhazmat.2019.02.057.

Kong, F., Parhiala, K., Wang, S., Fatehi, P., 2015. Preparation of cationic softwood kraft lignin and its application in dye removal. Eur. Polym. J. 67, 335–345. https://doi.org/10.1016/j.eurpolymj.2015.04.004.

Kontturi, E., Laaksonen, P., Linder, M.B., Nonappa, Gröschel, A.H., Rojas, O.J., Ikkala, O., 2018. Advanced materials through assembly of nanocelluloses. Adv. Mater. 30 https://doi.org/10.1002/adma.201703779.

Langmuir, I., 1918. The adsorption of gases on plane surfaces of glass, mica and platinum. J. Am. Chem. Soc. 40, 1361–1403.

Liu, Y., Liang, Z., Lin, C., Ye, X., Lv, Y., Xu, P., Liu, M., 2022. Insights into efficient adsorption of the typical pharmaceutical pollutant with an amphiphilic cellulose aerogel. Chemosphere 291, 132978. https://doi.org/10.1016/j.chemosphere.2021.132978.

Lv, Y., Liang, Z., Li, Y., Chen, Y., Liu, K., Yang, G., Liu, Y., Lin, C., Ye, X., Shi, Y., Liu, M., 2021. Efficient adsorption of diclofenac sodium in water by a novel functionalized cellulose aerogel. Environ. Res. 194, 110652 https://doi.org/10.1016/j.envres.2020.110652.

Moberg, T., Sahlin, K., Yao, K., Geng, S., Westman, G., Zhou, Q., Oksman, K., Rigdahl, M., 2017. Rheological properties of nanocellulose suspensions: effects of fibril/particle dimensions and surface characteristics. Cellulose 24, 2499–2510. https://doi.org/10.1007/s10570-017-1283-0.

Mozaffari Majd, M., Kordzadeh-Kermani, V., Ghalandari, V., Askari, A., Sillanpää, M., 2022. Adsorption isotherm models: a comprehensive and systematic review (2010−2020). Sci. Total Environ. 812 https://doi.org/10.1016/j.scitotenv.2021.151334.

Nanaki, S.G., Kyzas, G.Z., Tzereme, A., Papageorgiou, M., Kostoglou, M., Bikiaris, D.N., Lambropoulou, D.A., 2015. Synthesis and characterization of modified carrageenan microparticles for the removal of pharmaceuticals from aqueous solutions. Colloids Surf., B 127, 256–265. https://doi.org/10.1016/j.colsurfb.2015.01.053.

Österberg, M., Rojas, O.J., Sipponen, M.H., Mattos, B.D., 2020. Spherical lignin particles: a review on their sustainability and applications. Green Chem. 22, 2712–2733. https://doi.org/10.1039/d0gc00096e.

Pedrosa, M., Ribeiro, R.S., Guerra-Rodríguez, S., Rodríguez-Chueca, J., Rodríguez, E., Silva, A.M.T., Đolic, M., Rita Lado Ribeiro, A., 2022. Spirulina-based carbon biosorbent for the efficient removal of metoprolol, diclofenac and other micropollutants from wastewater. Environ. Nanotechnol. Monit. Manag. 18 https://doi.org/10.1016/j.enmm.2022.100720.

Pires, B.C., Dutra, F.V.A., Nascimento, T.A., Borges, K.B., 2017. Preparation of PPy/cellulose fibre as an effective potassium diclofenac adsorbent. React. Funct. Polym. 113, 40–49. https://doi.org/10.1016/j.reactfunctpolym.2017.02.002.

Qu, R. jing, Wang, Y., Li, D., Wang, L. jun, 2021. Rheological behavior of nanocellulose gels at various calcium chloride concentrations. Carbohydr. Polym. 274, 118660 https://doi.org/10.1016/j.carbpol.2021.118660.

Rajahmundry, G.K., Garlapati, C., Kumar, P.S., Alwi, R.S., Vo, D.V.N., 2021. Statistical analysis of adsorption isotherm models and its appropriate selection. Chemosphere 276, 130176. https://doi.org/10.1016/j.chemosphere.2021.130176.

Rashed, M.N., 2013. Adsorption Technique for the Removal of Organic Pollutants. Intech Open, p. 64. https://doi.org/10.5772/32009.

Rivera-Utrilla, J., Sánchez-Polo, M., Ferro-García, M.Á., Prados-Joya, G., Ocampo-Pérez, R., 2013. Pharmaceuticals as emerging contaminants and their removal from water. A review. Chemosphere 93, 1268–1287. https://doi.org/10.1016/j.chemosphere.2013.07.059.

Sipponen, M.H., Lange, H., Crestini, C., Henn, A., Österberg, M., 2019. Lignin for nano- and microscaled carrier systems: applications, trends and challenges. ChemSusChem 12, 2039–2054. https://doi.org/10.1002/cssc.201900480.

Sipponen, M.H., Smyth, M., Leskinen, T., Johansson, L.S., Österberg, M., 2017. All-lignin approach to prepare cationic colloidal lignin particles: stabilization of durable Pickering emulsions. Green Chem. 19, 5831–5840. https://doi.org/10.1039/c7gc02900d.

Sips, R., 1948. On the structure of a catalyst surface. J. Chem. Phys. 16, 490–495. https://doi.org/10.1063/1.1746922.

Skogberg, A., Mäki, A.J., Mettänen, M., Lahtinen, P., Kallio, P., 2017. Cellulose nanofiber alignment using evaporation-induced droplet-casting, and cell alignment on aligned nanocellulose surfaces. Biomacromolecules 18, 3936–3953. https://doi.org/10.1021/acs.biomac.7b00963.

Supanchaiyamat, N., Jetsrisuparb, K., Knijnenburg, J.T.N., Tsang, D.C.W., Hunt, A.J., 2019. Lignin materials for adsorption: current trend, perspectives and opportunities. Bioresour. Technol. 272, 570–581. https://doi.org/10.1016/j.biortech.2018.09.139.

Thiebault, T., Guégan, R., Boussafir, M., 2015. Adsorption mechanisms of emerging micro-pollutants with a clay mineral: case of tramadol and doxepine pharmaceutical products. J. Colloid Interface Sci. 453, 1–8. https://doi.org/10.1016/j.jcis.2015.04.029.

Tie, L., Ke, Y., Gong, Y., Zhang, W. xian, Deng, Z., 2022. Nanocellulose fine-tuned poly (acrylic acid) hydrogel for enhanced diclofenac removal. Int. J. Biol. Macromol. 213, 1029–1036. https://doi.org/10.1016/j.ijbiomac.2022.06.051.

UNESCO and HELCOM, 2017. Pharmaceuticals in the Aquatic Environment of the Baltic Sea Region: A Status Report. UNESCO Publishing, Paris.

von Schoultz, S., 2016. Method for Extracting Lignin. WO 2015104460.

Wang, J., Guo, X., 2020. Adsorption isotherm models: classification, physical meaning, application and solving method. Chemosphere 258, 127279. https://doi.org/10.1016/j.chemosphere.2020.127279.

Wang, T., Jiang, M., Yu, X., Niu, N., Chen, L., 2022. Application of lignin adsorbent in wastewater Treatment: a review. Separ. Purif. Technol. 302, 122116 https://doi.org/10.1016/j.seppur.2022.122116.

Zhu, G., Chen, Z., Wu, B., Lin, N., 2019. Dual-enhancement effect of electrostatic adsorption and chemical crosslinking for nanocellulose-based aerogels. Ind. Crop. Prod. 139, 111580 https://doi.org/10.1016/j.indcrop.2019.111580.